



Seven-year observation of multi-TeV gamma rays from the Crab Nebula with the Tibet air shower array

THE TIBET AS γ COLLABORATION

Abstract: The Tibet III air shower array, consisting of 533 scintillation counters which are placed in a lattice with 7.5 m spacing, has been in operation since 1999 at Yangbajing in Tibet, China at an altitude of 4,300 m above sea level. The systematic error in pointing accuracy of the Tibet III air shower array is estimated to be smaller than 0.011° , and the systematic error in the absolute energy scale is estimated to be less than approximately $\pm 8\%$ using the Moon's shadow. We observed multi-TeV gamma rays from the Crab Nebula with the Tibet III air shower array continuously. The gamma-ray energy spectrum from the Crab Nebula observed with the Tibet III air shower array is consistent with other observations by the imaging atmospheric Cherenkov telescopes.

Introduction

The Crab Nebula has been well studied with imaging atmospheric Cherenkov telescopes (IACTs) and has been established as a standard source in TeV gamma-ray astronomy [1] [2] [3].

In this paper we describe multi-TeV gamma-ray flux from the Crab Nebula observed with the Tibet III air shower array using seven-calendar-year data between 1999 and 2005. We also discuss our systematic errors, such as the pointing accuracy and the absolute energy scale, which have been checked by monitoring the Moon's shadow in the cosmic-ray flux.

Tibet Air Shower Array

The Tibet Air Shower array has been successfully operated since 1990 using well-established air shower techniques at Yangbajing (90.522°E , 30.102°N , 4300 m above sea level) in Tibet, China. The Tibet I array was constructed in 1990 [4] and it was gradually expanded to the Tibet II by 1994 which consisted of 185 fast-timing (FT) scintillation counters and 36 density (D) scintillation counters around the FT-counter array. From 1996 the array was upgraded again and the Tibet III was set

up in 1999 composed of 497 FT counters covering $36,900\text{ m}^2$ and 36 D counters around them. In the inner $22,000\text{ m}^2$, we deployed 429 FT counters with 7.5 m lattice interval, the rest of 68 FT counters with 15 m lattice interval, and 36 D counters with 30 m lattice interval around FT counter array. The array continued to be upgraded until 2003, and it consists of 761 FT counters, at present, covering $50,400\text{ m}^2$ and 28 D counters around them as shown in Fig. 1. With the Tibet air shower array, we have successfully observed a new cosmic-ray anisotropy in the Cygnus region at multi-TeV energies [5] as well as multi-TeV gamma rays from the Crab Nebula [6], Mrk501 [7] and Mrk421 [8] together with searches for multi-TeV new point sources in the northern sky [9], for multi-TeV diffuse gamma rays from the galactic plane [10], and for PeV gamma rays from point sources [11].

The observation of the Moon's shadows by a ground-based AS array is very useful to calibrate the performance of the AS array itself. Almost of primary cosmic rays are positively charged, they are bent westward by the geomagnetic field at Yangbajing, therefore, the position of the Moon's shadow shifts from the original Moon's position [12]. On the contrary, they are unaffected in the north-south direction as the east-west component of the geomagnetic field is negligible ($\sim 10\%$) at

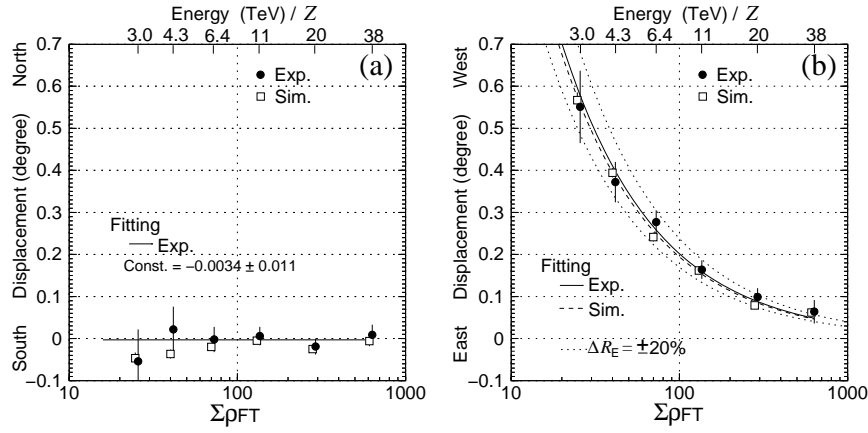


Figure 2: Shower size dependence of the displacement of the Moon's shadow in the north-south direction (a) and in the east-west direction (b). The closed circles show the experimental data, and the open squares represent the Moon's shadow simulation. The solid line in (a) shows the fitting to the experimental data assuming a constant function. The solid and dashed lines in (b) are fitted to the experimental data and the MC simulation data, respectively. Upper scale indicates the log-scale mean of rigidity (TeV / Z) in each $\Sigma\rho_{\text{FT}}$ bin.

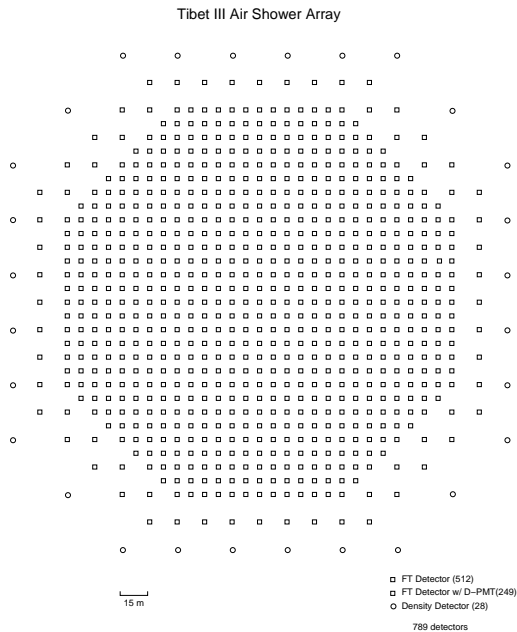


Figure 1: Tibet III air shower array.

Yangbajing. Since the geomagnetic field between the Earth and the Moon is accurately measured and modeled, and the energy spectrum and the composition of cosmic rays at < 100 TeV are measured by direct measurements, the observed position and the shape of the Moon's shadow enable us to calibrate the possible systematic error in the absolute energy scale (westward shift), angular resolution and absolute pointing (north-south direction) by multi-TeV primary cosmic-ray directions estimated by the AS event reconstruction procedure.

Figure 2 (a) shows the energy dependence of the displacement of the Moon's shadow in the north-south direction. A χ^2 fitting gives $0.0034^\circ \pm 0.011^\circ$ assuming a constant function independent of energy. From this, the systematic pointing error is estimated to be smaller than 0.011° .

Figure 2 (b) shows the shower size dependence of the displacement of the Moon's shadow in the east-west direction. In this figure, the open squares show the expected deflection, and a Monte Carlo (MC) simulation is quite consistent with the observational data. As a result, the systematic error in the absolute energy scale is estimated to be less than approximately $\pm 8\%$ level by means of the geomagnetic field as a spectrometer [13].

Analysis

In this paper, we only use data from 497 FT counters and 36 D counters set up by 1999 in order to keep the data consistency. A total of 2.0×10^{10} air shower events were collected during 1319 detector live days from November 18, 1999 to November 15, 2005 after the quality cut and the event selection based on the following simple criteria; (1) Air shower core location: Among the nine hottest counters in each event, eight should be contained in the inner 22,000 m². (2) Shower Size: Each shower event should fire four or more of 497 FT counters recording 1.25 particles or more, and $\Sigma\rho_{\text{FT}}$ should be more than 17.8 where $\Sigma\rho_{\text{FT}}$ is the sum of the number of particles per m² counted by the 497 FT counters. (3) Zenith angle: The zenith angle of the arrival direction should be less than 45°.

In order to extract an excess of TeV gamma-ray events coming from the direction of the Crab Nebula, the background event density must be carefully estimated. The background is estimated by the number of events averaged over eight off-source cells with the same angular radius as on-source, at the same zenith angle, recorded at the same time intervals as the on-source cell events. The search window radius is expressed as $6.9/(\Sigma\rho_{\text{FT}})^{0.5}$ degrees as a function of $\Sigma\rho_{\text{FT}}$, which maximizes the S/\sqrt{N} ratio according to a MC study. The center positions of these off-source cells, located at every 3.2° step from the source position measured in terms of angle distance in the azimuthal direction at the same zenith angle as the on-source direction. It is worthwhile here to note that two off-source cells adjacent to the on-source cell are excluded in order to avoid a possible signal tail leaking in the off-source events. This method, the so-called equi-zenith angle background estimation, can reliably estimate the background events under the same condition as on-source events. The Tibet III array, however, has a small anisotropy of $\pm 1.5\%$ in maximum amplitude in the azimuthal direction, as the array is constructed on the ground with a slight slope of +1.3° to the normal plane in the northwest direction. Hence, we analyzed 71 different dummy sources that follow the same diurnal rotation (at the same declination) as that of the Crab Nebula using the equi-zenith angle method

and corrected the anisotropy of off-source events using the azimuthal distribution averaged over 71 dummy sources events.

Results and Discussions

In order to determine the energy spectrum from the Crab Nebula, we calculated the detector response of the Tibet III array based on the full-MC simulation. For this, gamma rays from the Crab Nebula are simulated taking into account the diurnal motion of the Crab Nebula in the sky. Air shower events are uniformly thrown within a circle with a radius of 300 m whose center is positioned on the center of the array. This radius is sufficient to collect all gamma-ray events that are actually triggered in our array. Using the calculated effective area, the excess event rate, live time, and the relation between $\Sigma\rho_{\text{FT}}$ and the primary gamma-ray energy, we can calculate the differential energy spectrum of gamma rays from the Crab Nebula. In the present work, the energy points indicate the log-scale mean of energies in each $\Sigma\rho_{\text{FT}}$ bin defined as follows: $10 \times 10^{n/4} < \Sigma\rho_{\text{FT}} \leq 10 \times 10^{(n+1)/4}$ ($n = 1, 2, 3$), $100 \times 10^{n/3} < \Sigma\rho_{\text{FT}} \leq 100 \times 10^{(n+1)/3}$ ($n = 0, 1, 2$) and $\Sigma\rho_{\text{FT}} > 1000$. Thus, the total number of energy bins available in the analysis is seven. Figure 3 shows the differential energy spectrum of gamma rays from the Crab Nebula observed with the Tibet III array, together with those obtained by the IACTs. The energy spectrum obtained by the Tibet III is consistent with other observations by the IACTs.

Acknowledgements

The collaborative experiment of the Tibet Air Shower Arrays has been performed under the auspices of the Ministry of Science and Technology of China and the Ministry of Foreign Affairs of Japan. This work was supported in part by Grants-in-Aid for Scientific Research on Priority Area (712) (MEXT), by the Japan Society for the Promotion of Science, by the National Natural Science Foundation of China, and by the Chinese Academy of Sciences.

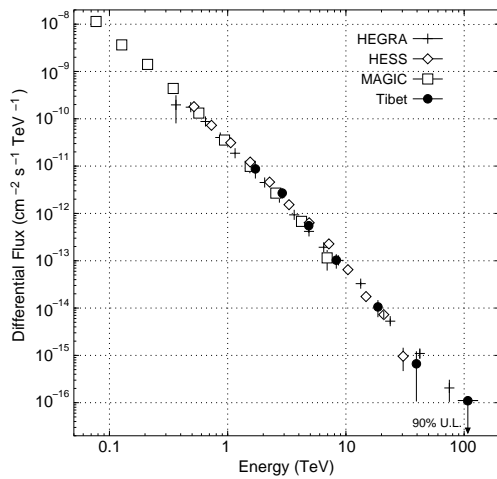


Figure 3: Differential energy spectrum of gamma rays from the Crab Nebula observed with the Tibet III array, together with those obtained by the IACTs, *i.e.*, HEGRA [1], HESS [2] and MAGIC [3].

References

- [1] F. Aharonian *et al.*, *ApJ.*, **614**, 897 (2004)
- [2] F. Aharonian *et al.*, *A. & A.*, **457**, 899 (2006)
- [3] J. Albert *et al.*, *astro-ph*, arXiv:0705.3244v1
- [4] M. Amenomori *et al.*, *Phys. Rev. Lett.*, **69**, 2468 (1992)
- [5] M. Amenomori *et al.*, *Science*, **314**, 439 (2006)
- [6] M. Amenomori *et al.*, *ApJ.*, **525**, L93 (1999)
- [7] M. Amenomori *et al.*, *ApJ.*, **532**, 302 (2000)
- [8] M. Amenomori *et al.*, *ApJ.*, **598**, 242 (2003)
- [9] M. Amenomori *et al.*, *ApJ.*, **633**, 1005 (2005)
- [10] M. Amenomori *et al.*, *ApJ.*, **580**, 887 (2002)
- [11] M. Amenomori *et al.*, *ApJ.*, **635**, L53 (2005)
- [12] M. Amenomori *et al.*, *Phys. Rev.*, **D47**, 2675 (1993)
- [13] M. Amenomori *et al.*, *Proc. of 29th ICRC*, **6**, 53 (2005)